sciendo | Nordic Concrete Federation

ISSN online 2545-2819
ISSN print 0800-6377

DOI: 10.2478/ncr-2025-0015

Received: April 6, 2024
Revision received: June 6, 2025
Accepted: June 10, 2025

A Hygrothermal Model to Simulate Moisture Conditions in Concrete Reactor Containments with Long-Term Temperature Gradients

Magnus Åhs, Ph.D.
Senior lecturer, Lund university
Box 118
221 00 Lund
magnus.ahs@byggtek.lth.se

ABSTRACT
Moisture plays a critical role in several degradation mechanisms affecting the structural components of nuclear power plants. It also significantly influences the long-term structural behaviour of reactor containments. This study presents a novel hygrothermal model that uses the relative humidity as the transport potential and accounts for the presence of a thermal gradient across the containment wall. The model is applied to predict moisture conditions in a concrete reactor containment after 30 years of operation. For evaluation, its predictions are compared with both long-term measurement data from a Swedish pressurised water reactor (PWR) and previously published results obtained using an established moisture transport model based on air vapour content. These published results demonstrate that the established model, while adequate under isothermal conditions, yields inaccurate predictions when a temperature gradient is present. In contrast, the proposed model shows good agreement with the measurement data. To capture thermal effects, the model incorporates novel methods for estimating the temperature dependence of sorption isotherms and moisture transport properties—an essential improvement when modelling moisture behaviour under non-isothermal conditions.

Key words: concrete, hygrothermal modelling, moisture transport, reactor containment, relative humidity

1. INTRODUCTION

1.1 Hygrothermal models

There are many hygrothermal models in the literature describing moisture transport under a temperature gradient in porous materials, e.g. [1-10]. Although these models simulate moisture transport in concrete under temperature gradients, they are often complex and require many input parameters. In contrast, the model proposed in this study offers a simplified yet effective hygrothermal formulation. It captures the essential mechanisms of moisture transport with minimal parameter input. The model comprises two governing equations—the energy conservation equation and the moisture transport equation—which are detailed in the following sections.

2. HYGROTHERMAL MODELLING

2.1 Heat transfer model

The heat transfer in the reactor containment, RC, is described by the energy conservation equation (1)

$$\rho \cdot C_p \cdot \frac{\partial T}{\partial t} + \rho \cdot C_p \cdot u \nabla T = \nabla(k \nabla T) + Q_1 \quad (1)$$

where ρ represents the density in [kg/m^3], C_p represents the heat capacity in [J/(kg K)], T represents the temperature in [K], t represents the time in [s], u may represent a convective flow but is here assumed to be zero, k represents the thermal conductivity in [W/(m K)] and Q_1 represents a heat source in [W/m^3]. The heat source may describe the heat released when the cement reacts with water. As the heat released from the chemical reactions is present only at a small fraction of the service life time span of a RC it is neglected.

In the simulated case, the density, heat capacity and thermal conductivity were considered constant and therefore neither affected by the temperature nor by the moisture content. They were assigned the values of 2350 [kg/m^3], 880 [J/(kg K)] and 1.4 [W/(m K)] respectively. This is of course a simplification.

2.2 Common method to model moisture transport

One common method for modelling one-dimensional moisture transport in concrete is described by Hedenblad [11], see equation (2)

$$J = -\delta_v \frac{\partial v}{\partial x} \quad (2)$$

where, J represents moisture transport in [kg/(m^{2}s)] with air vapour content as a driving potential, δ_v represents the diffusion coefficient in [m^2/s] and v represents vapour content in the pores [kg/m^3].

Such a model of moisture transport is valid for moisture transport driven by vapour content at a constant temperature. Despite the fact that it is valid for a constant temperature, this transport model was used by Nilsson and Johansson to simulate the moisture distribution in a concrete RC wall [12, 21], where a temperature gradient was present. The temperature [°C] and vapour content [kg/m^3] in the RC wall are presented in Figure 1 and Figure 2, respectively. Note that the black thick vertical solid line represents the steel liner, impermeable to moisture transport. The depth is measured from the outdoor surface.

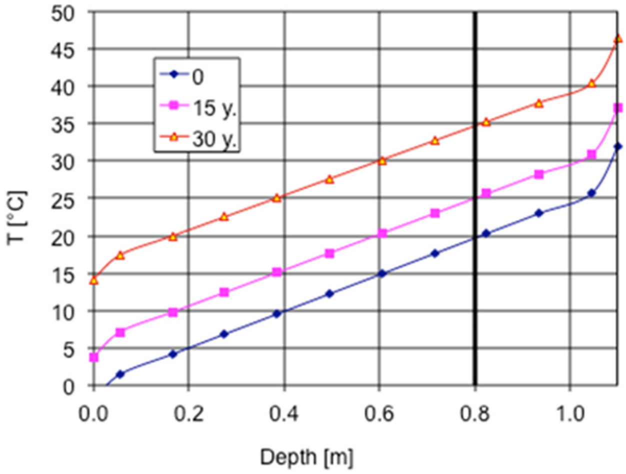

Figure 1 – Temperature distribution in RC wall at year 0, 15 and 30, simulations performed by Nilsson and Johansson [12, 21].

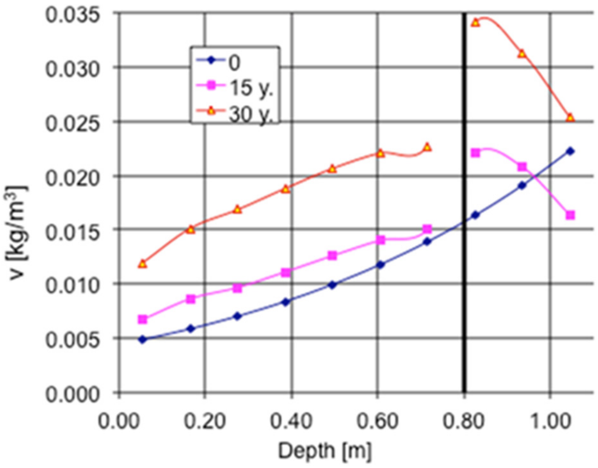

Figure 2 – Vapour content distribution in RC wall at year 0, 15 and 30, simulations performed by Nilsson and Johansson [12, 21].

The vapour content distribution was given by the suggested initial *RH* that was set as a nearly uniform distribution, see Figure 3. The moisture transport model gave the following results in terms of relative humidity, *RH*, and evaporable moisture content, *W*, which are presented in Figure 3 and Figure 4, respectively.

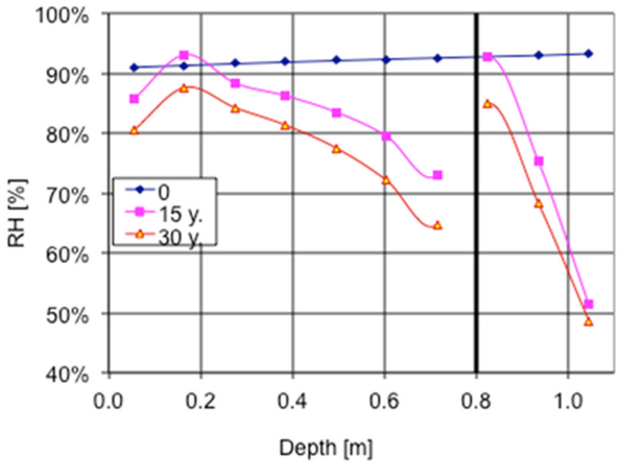

Figure 3 – RH distribution in RC wall at year 0, 15 and 30, simulations performed by Nilsson and Johansson [12, 21].

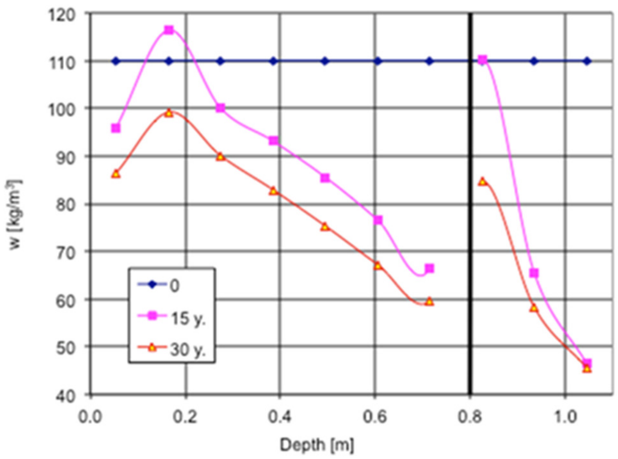

Figure 4 – Evaporable moisture content distribution, W, in RC wall at year 0, 15 and 30, simulations performed by Nilsson and Johansson [12, 21].

The predicted moisture content shown in Figure 4 implies that the concrete RC wall is more humid about 0.18 m from the out door surface and less humid at the steel liner. This suggests that moisture is drying through the steel liner, which is unlikely as the steel liner is regarded as impermeable to moisture.

Moisture profiles determined in RC walls from pressure water reactors, PWRs which have been in operation for a long time are scarce. Such walls have been exposed to a large temperature gradient. One major reason for the scarcity is the unwillingness to penetrate the concrete wall by drilling. The owners do not want to take a risk of damaging the tendons and reinforcement steel. However, there is two moisture profiles that has been determined in RC walls of a PWR. This moisture measurement was performed after about 30 years of operation by Oxfall et al. [13]. The measurements were performed on samples from a 300 mm concrete core. Figure 5 shows the degree of capillary saturation, S_{cap}, evaluated from two separate samples of a concrete RC wall in a Swedish PWR that has been in operation more than 30 years, with a rather large and fairly constant temperature gradient of about 30°C. The solid line with square markers and the solid line with circles represent two different samples.

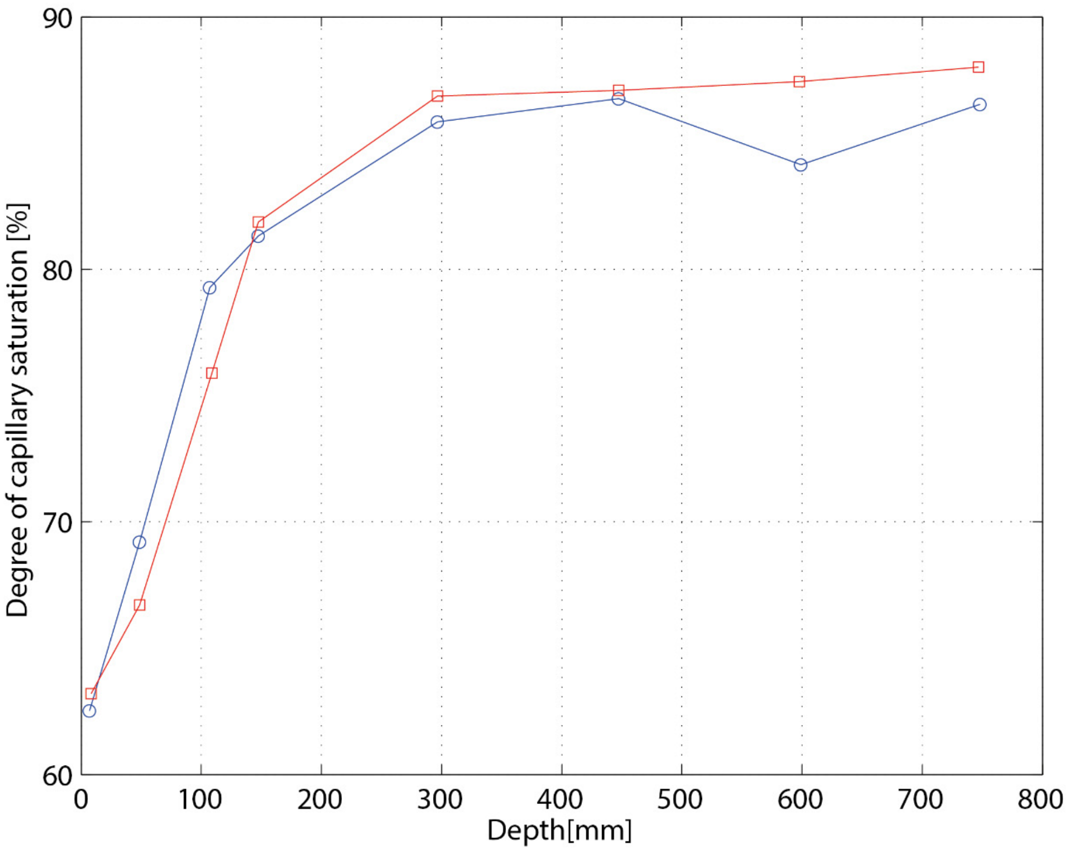

Figure 5 – Degree of capillary saturation distribution in a RC wall from a PWR, Ringhals 4, in Sweden, [13]. The depth is measured from the exterior surface. A steel liner is located at 800 mm.

These measurements clearly demonstrate that that equation (2) is not suitable for describing moisture transport under a temperature gradient. The S_{cap} determined after 30 years of operation shows that the moisture content is highest near the steel liner. S_{cap} represents the evaporable moisture content in relation to the moisture content at saturation. This implies that the highest evaporable moisture content level is located close to the steel liner. Consequently, using water vapour content as a transport potential under such thermal conditions is inappropriate. The attempt by Nilsson and Johansson [12] to simulate moisture transport by was therefore unsuccessful as the evaporable moisture content in the left part of Figure 4 and the S_{cap} in Figure 5 should have a similar shape of moisture distribution to be a proper model.

2.3 Suggested moisture transport model

Instead of using the vapour content as the moisture transport potential this model is using the relative humidity as a transport potential. The moisture transport in the proposed model is based on the mass conservation equation, equation (3),

$$\frac{\partial W_e}{\partial t} = \frac{\partial \mathrm{W_e}}{\partial RH}\frac{\partial RH}{\partial \mathrm{t}} = \nabla(\delta_{RH}\nabla RH) + Q_2 \tag{3}$$

where $\frac{\partial W_e}{\partial RH}$ represents the moisture capacity in [kg/m³], RH represents the relative humidity in [-], δ_{RH} is the moisture transport coefficient with RH as the driving potential in [m²/s·kg/m³], and Q_2 is a term representing a source or sink in [kg/m³]. The sink may represent self-desiccation. For simplicity, the simulations are initiated one year after the completion of the RC structure. At this stage, self-desiccation is considered to be largely complete and therefore insignificant. The internal relative humidity is assumed to be approximately 92% throughout the concrete. This uniform initial condition is deemed reasonable, as moisture exchange at the surfaces has only a limited influence on the internal relative humidity over the timescales considered.

Moisture capacity, which is needed in the model, is evaluated from the desorption isotherm of the concrete at the actual relative humidity level. The desorption isotherm used in this model is adopted from [12], see Figure 6.

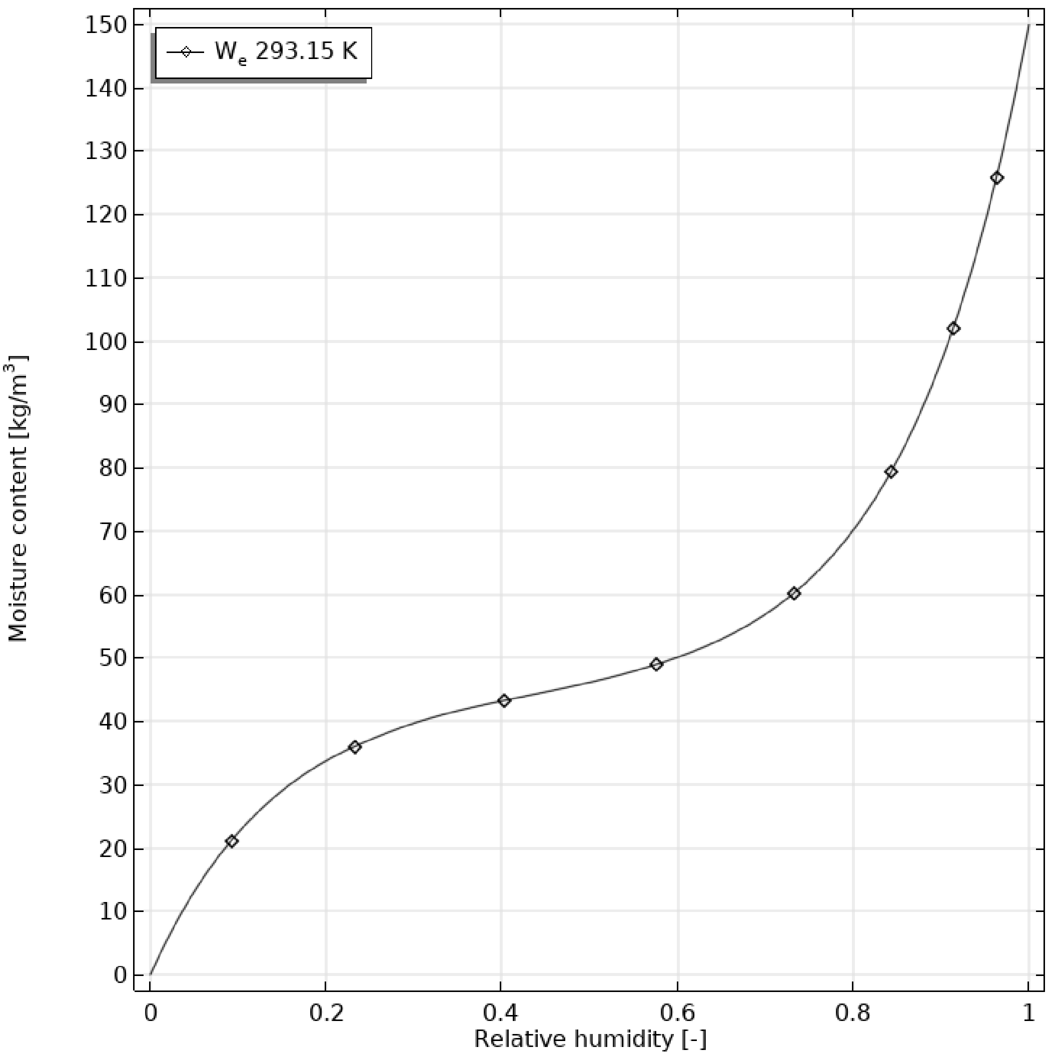

Figure 6 – The desorption isotherm shown at a temperature of 293.15 K [12].

The x-axis shows the RH in [-] and the y-axis shows the evaporable moisture content in [kg/m³]. However, as there is a temperature gradient present in the RC wall the basic sorption isotherm is not valid throughout the wall cross section. To account for the influence of temperature, the desorption isotherm was modified by superimposing a sinusoidal function, resulting in a temperature-dependent evaporable moisture content, denoted as, W_{eT}. The sinusoidal form was selected because it yields zero deviation at both ends of the relative humidity range (0% and 100%), thereby preserving the original moisture content at these extremes. The main adjustment occurs around 50% relative humidity, where the effect of temperature on sorption behaviour is most pronounced. This was accomplished by using equation (4),

$$W_{eT} = \left(\frac{293.15-T}{2}\right) \cdot \sin(RH \cdot \pi); \quad 0 < RH < 1; \;\; 273K < T < 323K \tag{4}$$

where, T is the temperature in [K], RH is the relative humidity in [-]. The sorption isotherms, W_{eT}, for 283.15 K, 293.15 K, and 313.15 K are shown in Figure 7.

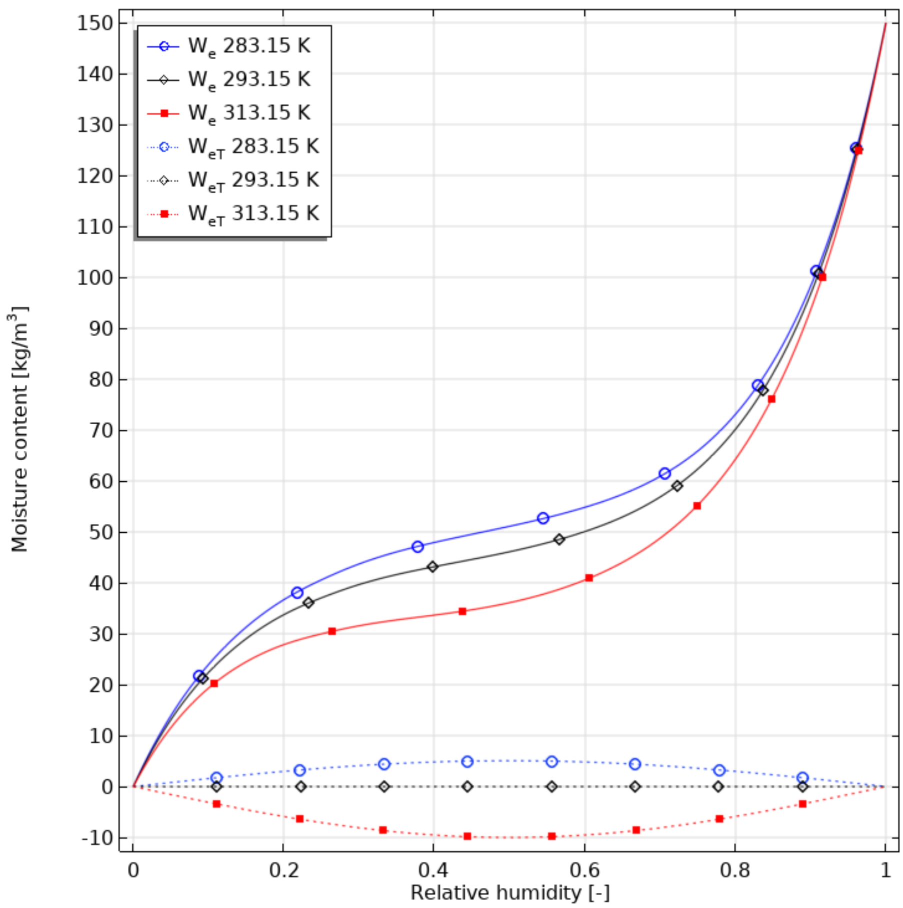

Figure 7 – Sorption isotherms, W_e, and the superimposed W_{eT}, shown at three different temperatures 283.15K, 293.15K and 313.15K.

Note the decrease in evaporable moisture content when the temperature increases, see red solid line in Figure 7, and the increase of the evaporable moisture content when the temperature decreases, see blue solid line in Figure 7. Sorption isotherms of concrete and cement paste at different temperatures have been presented in a few publications [14-18]. The suggested change of evaporable water with respect to temperature is of the same order of magnitude as presented by Poyet, [14].

The temperature dependent moisture transport coefficient, δ_{RH}, was modelled by using equation (5),

$$\delta_{RH} = \delta_v \cdot v_s \quad (5)$$

where, δ_v represents the vapour diffusion coefficient in [m^2/s], and v_s represents the saturation vapour content in [kg/m^3]. As the saturation vapour content is temperature dependent so is the δ_{RH}. The vapour diffusion coefficient, δ_v, was curve fitted to data presented in [11] by using equation (6),

$$\delta_v = 1.4 \cdot 10^{-7} \cdot e^{a \cdot RH^b} \quad (6)$$

where, a, and, b, are dimensionless constants. In this case they attained a value of 5, and 8, respectively.

The vapour saturation content, v_s, in [kg/m^3] was estimated by using equation (7) [19],

$$v_s = 1 \cdot 10^{-3} \cdot e^{\left(20.111 - \frac{5060.73}{T}\right)}, \ 273.15K < T < 323.15K \quad (7)$$

where, T represents the temperature in [K].

Moisture transport coefficients, δ_{RH}, are shown in Figure 8, at three different temperatures 283.15K, 293.15K and 313.15K.

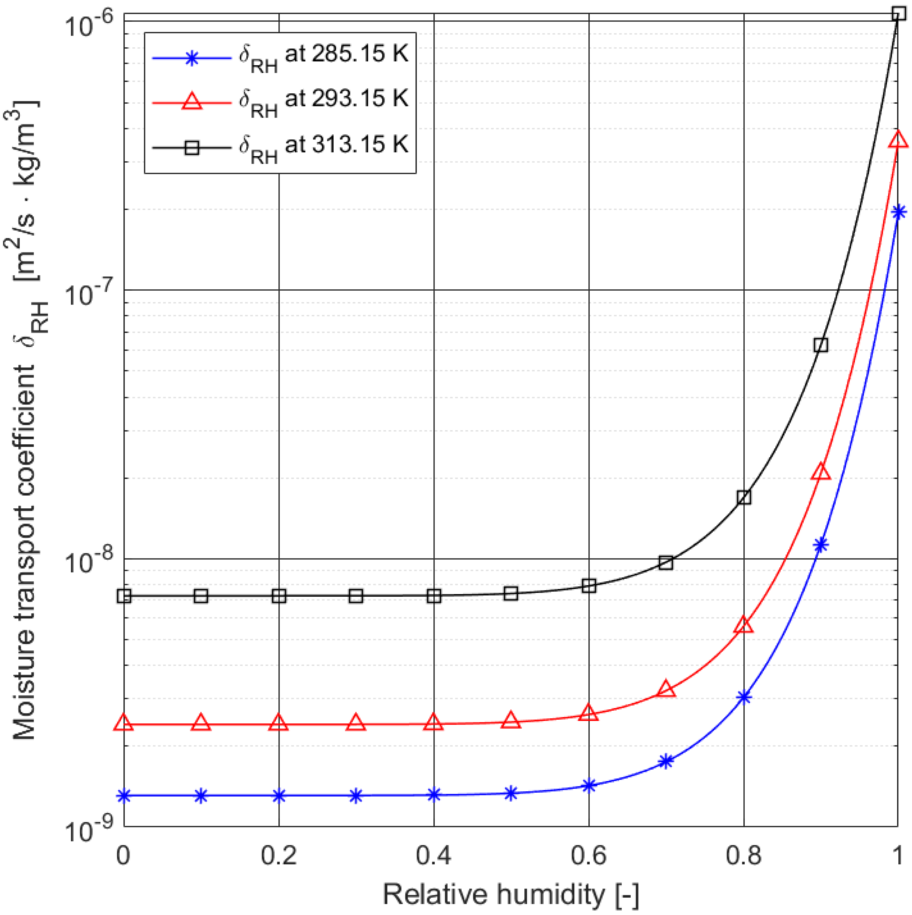

Figure 8 – The moisture transport coefficient, δ_{RH}, at three different temperatures 283.15K, 293.15K and 313.15K.

3. APPLICATION ON A REACTOR CONTAINMENT

The hygrothermal model was applied on a full scale 3D model of a real RC shown in Figure 9.

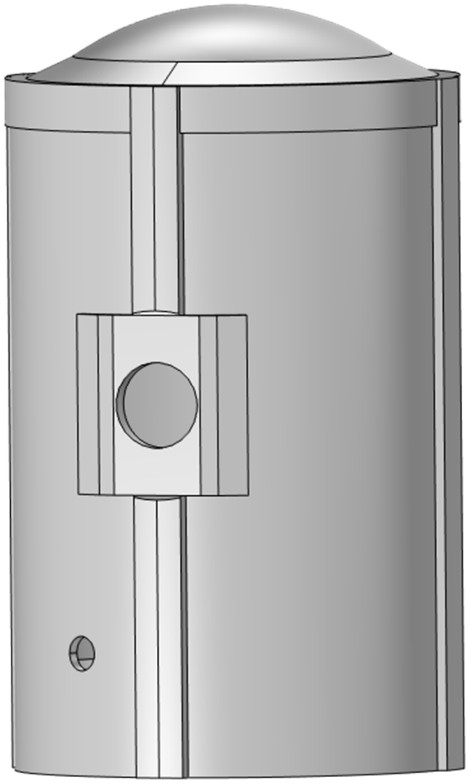

Figure 9 – Geometry of the reactor containment, about 66 m high and a radius of about 20 m.

The finite element mesh consisted of around 50 k tetrahedrons, 63 k prisms and 121 k elements in total. Linear solid elements with full integration were used. The mesh was created by using COMSOL Multiphysics option "free tetrahedral", which results in an unstructured mesh. This resulted in around 365 k degrees of freedom. Boundary layers were used at the inner surface of the foundation and the external surfaces.

The initial *RH* condition was set to 92% RH throughout the concrete volume, as a result of an assumed initial self-desiccation.

Minor details like tendons and reinforcement bars were excluded from the geometry in the hygrothermal simulation. This simplification was considered to have a limited impact on the overall moisture conditions. Inner surfaces of the containment wall, the surfaces of the three openings and the inner part of the dome were modelled as completely moisture impermeable. In reality these surfaces were covered with a steel lining. A convective boundary condition was prescribed, representing a flux across the surface governed by a transfer coefficient and a finite surface resistance. Where the moisture surface resistance, h_{RH}, was formulated according to Lewis relation [20], see equation (8),

$$h_{RH} = \frac{h_T \cdot v_s}{\rho_{air} \cdot C_{p(air)}} \tag{8}$$

where, h_T represents the heat transfer coefficient, v_s represents the saturation vapour content of air, ρ_{air} represents the density of air, and, $C_{p(air)}$ represents the specific heat capacity of air 1000 J/(kg K).

The RC that was simulated is located in the northwestern part of France. Climatic data from that geographical area served as a guide to generate the outdoor climate. The temperature and relative humidity for the indoor and outdoor climate were constructed as a sinusoidal annual variation; daily variations and rain were disregarded, by using these four equations (9)-(12),

$$RH_{indoor} = 0.3 + .035 \cdot \sin\left(\frac{2 \cdot \pi \cdot t}{3600 \cdot 24 \cdot 365}\right) \tag{9}$$

$$RH_{outdoor} = 0.8 + .08 \cdot sin\left(\frac{2 \cdot \pi \cdot t}{3600 \cdot 24 \cdot 365}\right) \tag{10}$$

$$T_{indoor} = 296 + \sin\left(\frac{2 \cdot \pi \cdot t}{3600 \cdot 24 \cdot 365}\right) + \frac{20 \cdot y}{66.4} \tag{11}$$

$$T_{outdoor} = 280 + 9 \cdot \sin\left(\frac{2 \cdot \pi \cdot t}{3600 \cdot 24 \cdot 365}\right) \tag{12}$$

where, t represents time in seconds and y represents hight from the base level in [m]. The equations for the indoor climate were chosen by the guidance of actual measurements performed in a Swedish PWR [21].

There are of course other factors that have an impact on the boundary conditions such as solar radiation, wind speed and direction, and the impact of the surroundings, moisture conditions below the foundation et cetera. However, these factors were disregarded in order reduce the complexity of the simulation.

4. SIMULATION RESULTS AND DISCUSSION

The hygrothermal model was solved using the finite element software COMSOL Multiphysics [22], version 6.3, which is capable of solving coupled partial differential equations. Such a tool is needed as both the moisture transport coefficient, and the sorption isotherm are dependent on the temperature. Figure 10 illustrates the *RH* distribution at four time points: 1, 10, 20 and 30 years after the commencement of the simulations at a height of 21 metres. Figure 11 illustrates the temperature distribution at the same time intervals as the *RH* distribution.

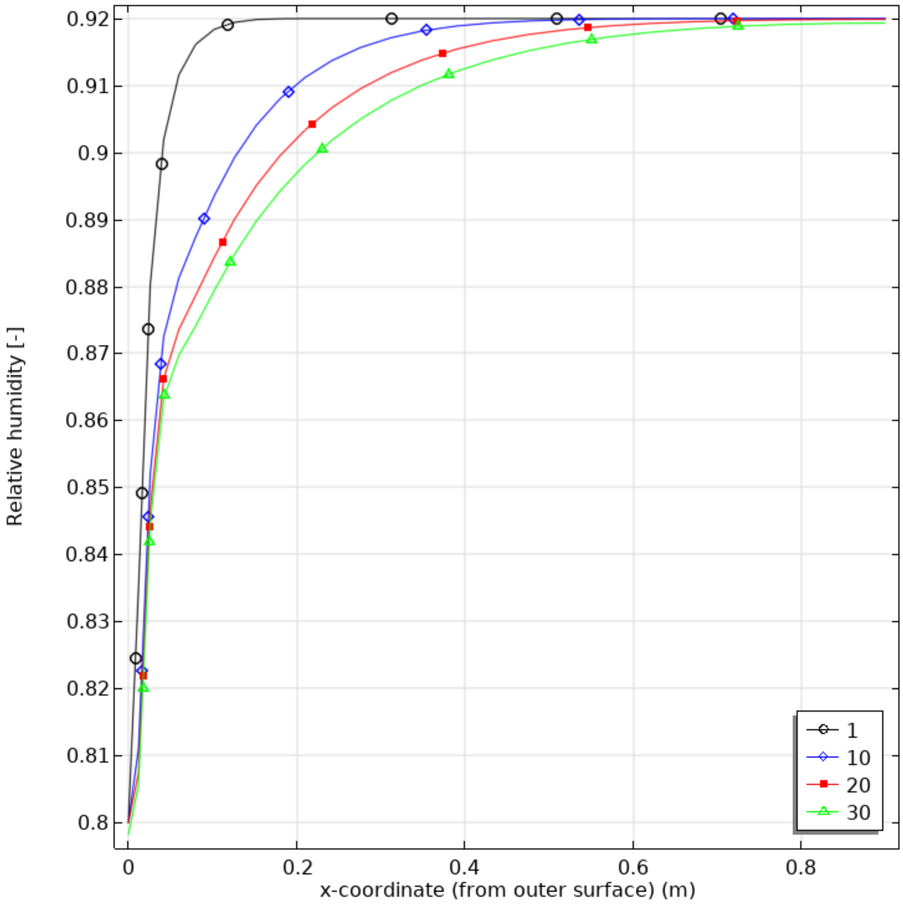

Figure 10 – Relative humidity distribution from a 1D cross section at 21 m above floor level of the 900 mm thick RC wall after 1, 10, 20 and 30 years in operation.

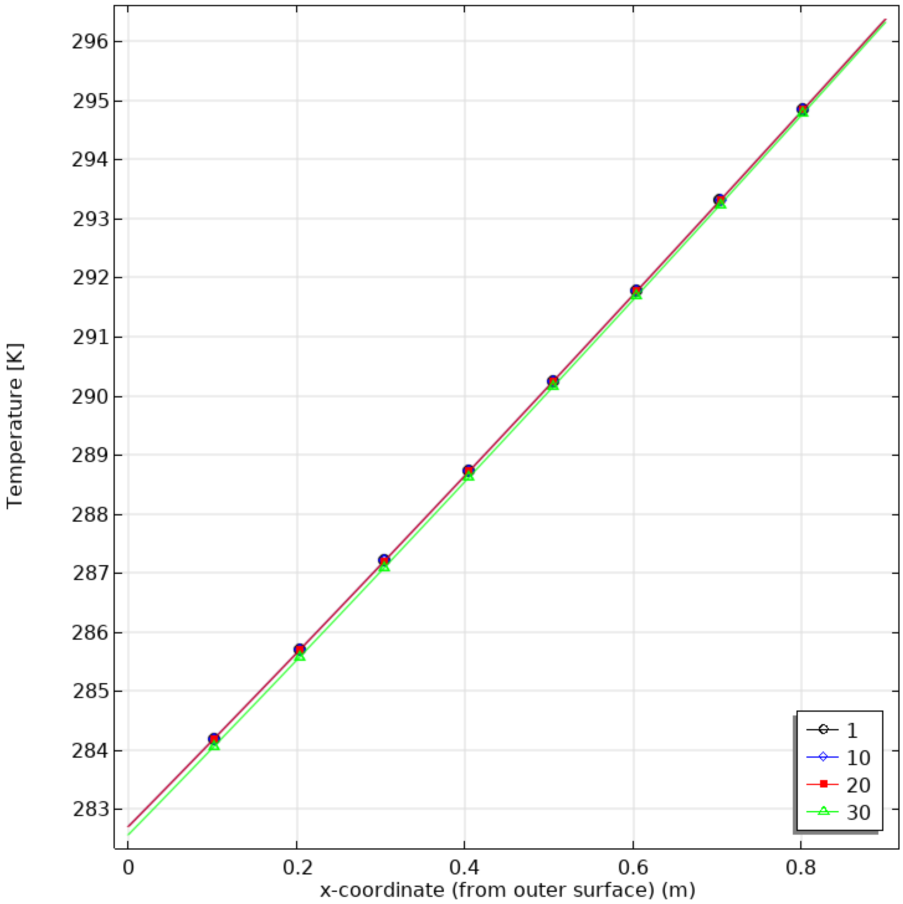

Figure 11 – Temperature distribution from a 1D cross section at 21 m above floor level of the 900 mm thick RC wall after 1, 10, 20 and 30 years in operation.

In Figure 12, the moisture content distribution in the RC wall is presented at the same points of time as the *RH* and temperature distributions, in Figures 10 and 11.

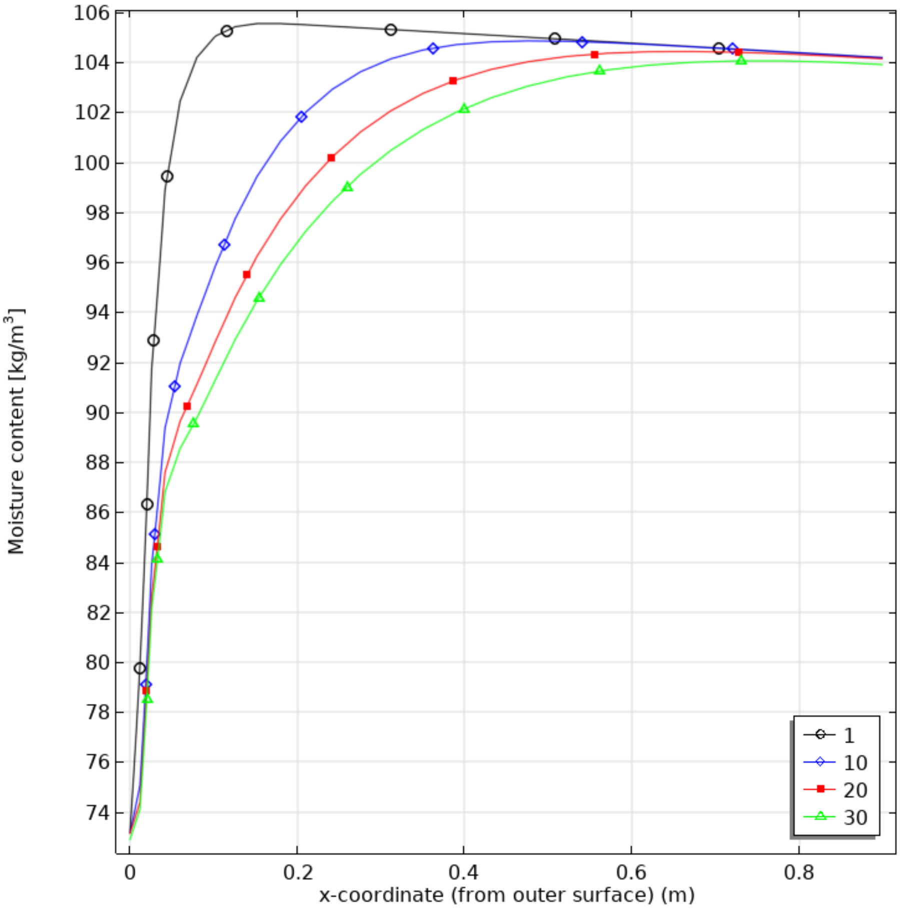

Figure 12 – Moisture content distribution from a 1D cross section at 21 m above floor level of the 900 mm thick RC wall after 1, 10, 20 and 30 years in operation.

The moisture content distribution after one year of operation is affected by the fact that a uniform *RH* at 92% was suggested as an initial value. This suggestion and the sorption isotherms temperature dependency give a moisture content distribution that is slightly higher at the outer surface (around 106 kg/m^3) than at the inner surface (around 104 kg/m^3). That initial suggestion has an impact throughout the simulation time of 30 years. A more refined initial moisture condition of the concrete would have resulted in a constant W_e. Nevertheless, the simulation results after approximately 30 years yield a moisture content distribution that closely aligns with the measurements conducted by Oxfall in [13]. This implies that it is much better to use the suggested hygrothermal model described in this paper than the model suggested by Nilsson in [21].

In Figures 13 and 14 the relative humidity and temperature distributions are shown of a cross section near the foundation of a RC after 30 years in operation. The thickness of the RC wall and foundation are 1.1 m and 3.5 m, respectively. The colour legends in Figures 13 and 14, represent the relative humidity in [-] and temperature in [K], respectively.

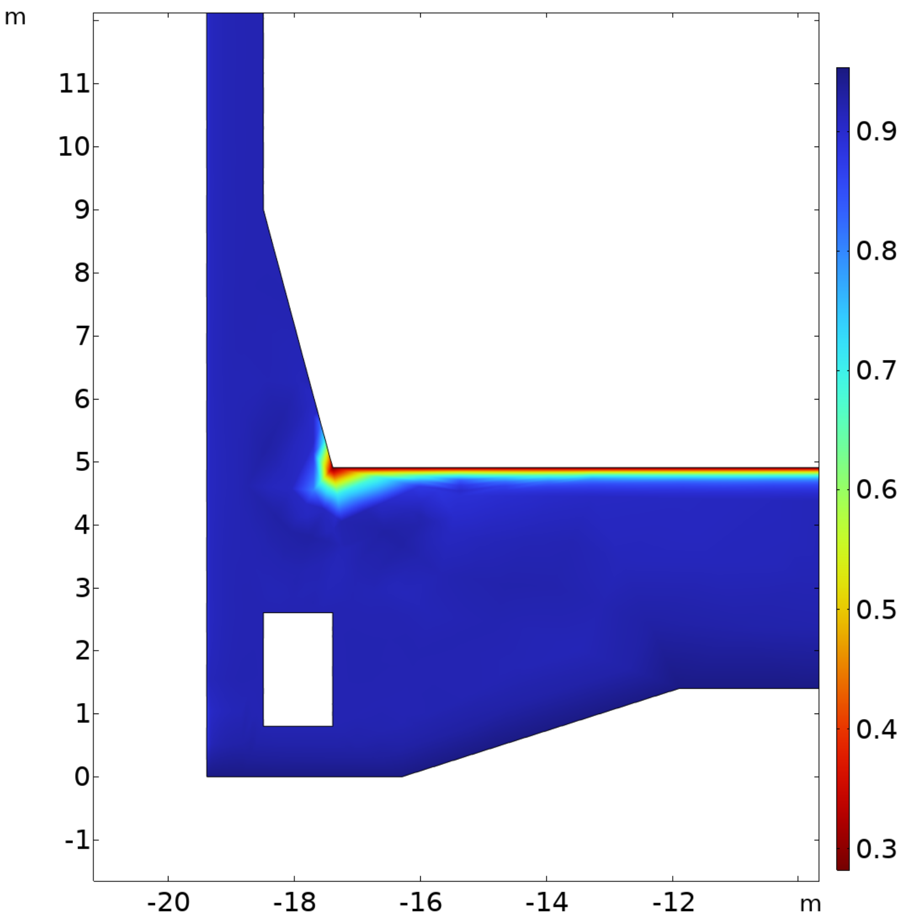

Figure 13 – Relative humidity distribution [-] at a 2D cross section near the foundation of the RC after 30 years of operation.

It is clear that the *RH* at the interior floor has dried because of the dry inner climate condition which is about 30 % RH. It is also clear that a major part of the concrete in the RC is not dried at all, see Figure 13. Interior parts of the wall have not dried at all since they are covered by a steel plate which is impermeable of moisture. The dry area close to the corner between the wall and slab is a result from the coarse mesh.

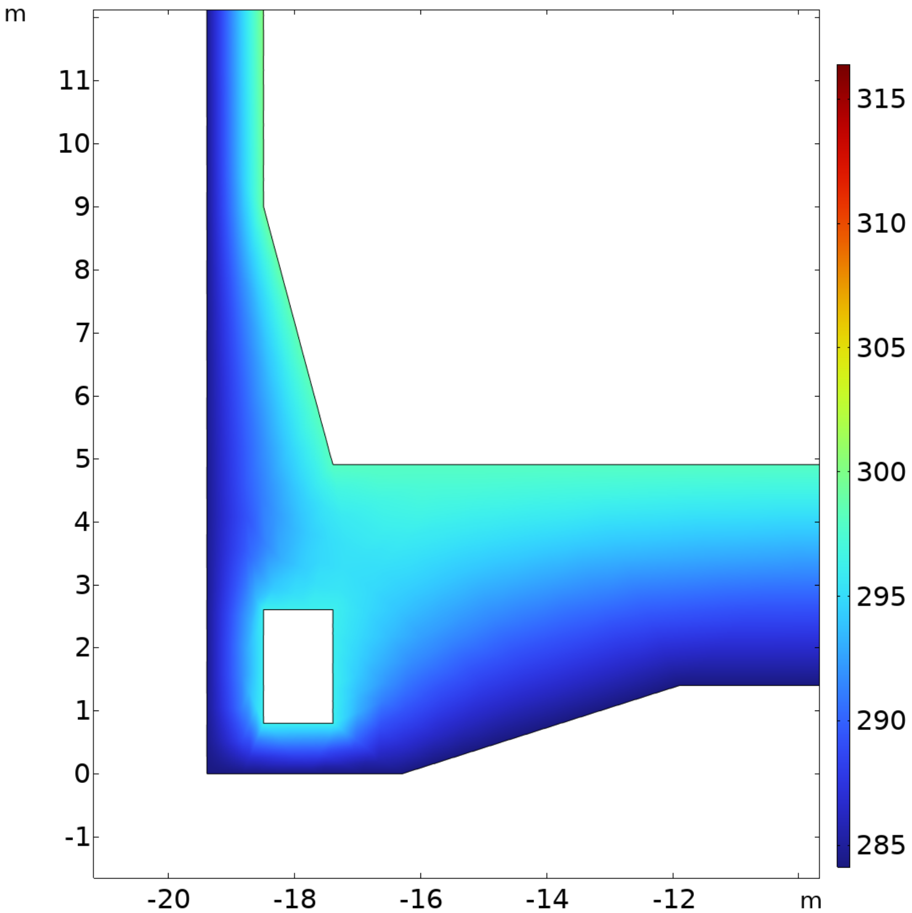

Figure 14 – Temperature distribution [K] at a 2D cross section near the foundation of the RC after 30 years of operation.

The temperature outside of the RC is clearly affected by the outdoor climate and this is clearly shown in Figure 14. It is also clear that the temperature in the RC is affected throughout the whole concrete volume by the boundary conditions.

Unfortunately, it was not possible to compare the results from the simulations with actual measurements performed on the real RC situated in France.

4. CONCLUSION

It was concluded that the proposed hygrothermal model is suitable for estimating the prevailing moisture conditions within the containment wall of a pressurised water reactor (PWR). The simulated moisture content distribution demonstrated good agreement with empirical measurements obtained from an actual RC structure in Sweden. This consistency between measured and simulated data supports the model's validity and its potential application in assessing long-term moisture behaviour in nuclear RCs subjected to thermal gradients.

ACKNOWLEDGEMENTS

NUGENIA/ACCEPPT and EDF (Electricité de France) are gratefully acknowledged for the financial support of this research. Lars-Olof Nilsson, Stéphane Poyet, and Valérie L'Hostis are gratefully acknowledged for their contributions to this study.

REFERENCES

1. Ishida, T., K. Maekawa, and T. Kishi: "Enhanced modeling of moisture equilibrium and transport in cementitious materials under arbitrary temperature and relative humidity history". *Cement and Concrete Research,* 2007. 37(4), pp. 565-578.
2. Lu, X.S: "Modelling of heat and moisture transfer in buildings - II. Applications to indoor thermal and moisture control". *Energy and buildings*, 2002. 34(10): pp. 1045-1054
3. Norling Mjörnell, K.: "Moisture Conditions in High Performance Concrete. Mathematical Modelling and Measurements", 1997, Institutionen för byggnadsmaterial, Chalmers tekniska högskola.
4. Obeid, W., G. Mounajed, and A. Alliche: "Mathematical formulation of thermo-hygro-mechanical coupling problem in non-saturated porous media". *Computer Methods in Applied Mechanics and Engineering*, 2001. 190(39), pp. 5105-5122.
5. Qin, M., et al.: "Nonisothermal moisture transport in hygroscopic building materials: modeling for the determination of moisture transport coefficients". *Transport in Porous Media,* 2008. 72(2), pp. 255-271.
6. Qin, Y. and J.E. Hiller: "Simulating moisture distribution within concrete pavement slabs: model development and sensitivity study". *Materials and Structures*, 2014. 47(1-2), pp. 351-365.
7. T. G. Myers, T.G. and J.P.F. Charpin: "Modelling the temperature, maturity and moisture content in a drying concrete block". *Mathematics-in-Industry Case Studies Journal*, 2008. Vol 1, pp. 24-48.
8. Holm, A.H. and H.M. Kuenzel: "Practical application of an uncertainty approach for hygrothermal building simulations-drying of an AAC flat roof". *Building and Environment*, 2002. 37(8-9): pp. 883-889
9. Du, M. , Xianyu Jin, Hailong Ye, Nanguo Jin, Ye Tian: "A coupled hygro-thermal model of early-age concrete based on micro-pore structure evolution". *Construction and Building Materials*, Vol. 111, 2016, pp. 689-698.
10. Veselý, J., Vít Šmilauer: "Hygro-thermo-mechanical model for concrete pavement from an early age to a long-term performance". *Construction and Building Materials*, Vol. 403, 133068, 2023.
11. Hedenblad, G: "Moisture permeability of mature concrete, cement mortar and cement paste". 1993, Div. of Building Materials, Lund University
12. Nilsson, L.-O.: "Moisture Transport Under A Temperature Gradient – Some Old And New Studies". 2013, Understanding the fundamental properties of concrete. Celebrating Professor Erik J. Sellevold on his 75th birthday, pp. 1-14.
13. Oxfall, M., P. Johansson, and M. Hassanzadeh: "Moisture profiles in concrete walls of a nuclear reactor containment after 30 years of operation". *Proceedings*, XXII Nordic

Concrete Research Symposium, 2014. Reykjavik, Iceland. Norsk Betongforening, pp. 479-482.

14. Poyet, S: “Experimental investigation of the effect of temperature on the first desorption isotherm of concrete”. *Cement and Concrete Research*, 2009. 39(11): pp. 1052-1059.
15. Daian, J.F.: “Condensation and isothermal water transfer in cement mortar Part I - Pore size distribution, equilibrium water condensation and imbibition”. *Transport in Porous Media, 1988*. 3(6), pp. 563-589.
16. Wu, M., B. Johannesson, and M. Geiker: “A study of the water vapor sorption isotherms of hardened cement pastes: Possible pore structure changes at low relative humidity and the impact of temperature on isotherms”. *Cement and Concrete Research*, 2014. 56: pp. 97-105.
17. Brue, F., et al.: “Effect of temperature on the water retention properties of two high performance concretes”. *Cement and Concrete Research*, 2012. 42(2), pp. 384-396.
18. Poyet, S., J-L Adia, S. Michel-Ponnelle: “Experimental characterisation of the isosteric desorption energy of VeRCoRs concrete: Comparison of the isotherms and hygrometric methods”. *Cement and Concrete Research*, Vol. 184, 2024, 107627.
19. Nilsson, L.O., Betonghandbok: Material, utgåva 2, Kapitel 14 Fukt och betong 1994: Svensk byggtjänst.
20. Lewis, W: “The evaporation of a liquid into a gas”. *International Journal of Heat and Mass Transfer*, 1962. 5(1-2): pp. 109-112.
21. Nilsson, L.O. and P. Johansson: ”Förändringsprocesser i reaktorinneslutningar Betongväggarnas klimatförhållanden och uttorkning”. Elforsk rapport 09:100, 2009. (In Swedish).
22. COMSOL, COMSOL Multiphysics Reference Manual, Version 6.3, COMSOL Inc. 2024